

Mn, Cu, etc.) oxide spinel structures in condensation and soluble polyimides are being pursued. Process parameters are also being probed to optimize the air-side oxide thickness, uniformity, and purity and to establish general structure-property-process correlations for metal ion modified polyimides. The model is being further probed by optical and electron microscopy and will be evaluated using ac electrical measurements.

**Acknowledgment.** We gratefully acknowledge the National Aeronautics and Space Administration for sponsoring this research, Leslie Horning for preparation of codoped films, Frank Cromer for his expertise and patience in performing the surface analysis, and Dr. Larry C. Burton (VPI & SU, Department of Electrical Engineering) for helpful suggestions and comments.

**Registry No.** BDTA-ODA polymer entry, 24980-39-0; BDTA-ODA SRU entry, 24991-11-5; Co, 7440-48-4; Li, 7439-93-2.

## References and Notes

- (1) Furtsch, T. A.; Taylor, L. T.; Fritz, T. W.; Fortner, G.; Khor, E. *J. Polym. Sci., Polym. Chem. Ed.* **1982**, *20*, 1287.
- (2) Ezzell, S. A.; Taylor, L. T. *Macromolecules* **1984**, *17*, 1627.
- (3) Boggess, R. K.; Taylor, L. T. *J. Polym. Sci., Polym. Chem. Ed.*, in press.
- (4) Rancourt, J. D.; Boggess, R. K.; Taylor, L. T. *Polym. Mater. Sci. Eng.* **1985**, *53*, 74.
- (5) Khor, E.; Taylor, L. T. *Macromolecules* **1982**, *15*, 379.
- (6) Rancourt, J. D.; Boggess, R. K.; Horning, L. S.; Taylor, L. T. *J. Electrochem. Soc.*, in press.
- (7) Appandairajan, N. K.; Viswanathan, B.; Gopalakrishnan, J. *J. Solid State Chem.* **1981**, *40*, 117.
- (8) Koumoto, K.; Yanagida, H. *J. Am. Ceram. Soc.* **1981**, November, C-156.
- (9) Rancourt, J. D.; Taylor, L. T. *Polym. Mater. Sci. Eng.* **1986**, *54*, 124.
- (10) Rancourt, J. D.; Swartzentruber, J. L.; Taylor, L. T. *Am. Lab. (Fairfield, Conn.)* **1986**, March.
- (11) St. Clair, A. K.; Taylor, L. T. *J. Appl. Polym. Sci.* **1983**, *28*, 2393.
- (12) Taylor, L. T.; St. Clair, A. K. *Polyimides*; Mittal, K. L., Ed.; Plenum: New York, 1984; Vol. 2; p 617.
- (13) *Instruction Manual*, Model 6105 Resistivity Adapter; Keithley Instruments: Cleveland, OH.
- (14) Sacher, E. *IEEE Trans. Electr. Insul.* **1979**, *EI-14* (2), 85.
- (15) Hanscomb, J. R.; Calderwood, J. H. *J. Phys. D.* **1973**, *6*, 1093.
- (16) Sacher, E.; Susko, J. R. *J. Appl. Polym. Sci.* **1979**, *23*, 2355.
- (17) Barker, R. E., Jr. *Pure Appl. Chem.* **1976**, *46*, 157.
- (18) Barker, R. E., Jr.; Sharbaugh, A. H. *J. Polym. Sci., Part C*, **1965**, *10*, 139.
- (19) Taylor, C. P. S. *Nature (London)* **1961**, *189*, 388.
- (20) Rancourt, J. D.; Taylor, L. T. *J. Therm. Anal.*, in press.
- (21) Warfield, R. W. *Treatise on Analytical Chemistry*; Kolthoff, I. M. et al., Eds.; Wiley: New York, 1977; Vol. 4, Part III, p 615.
- (22) Appandairajan, N. K.; Gopalakrishnan, J. *Proc. Indian Acad. Sci., Sect. A* **1978**, *87A*, 115.
- (23) Rao, C. N. R.; Rao, G. V. S. *Transition Metal Oxides*; National Bureau of Standards; Gaithersburg, MD, 1972; NSRDS-NBS 49.

## Study of Mobile and Rigid Peroxy Radicals in Polypropylene

M. G. Alonso-Amigo and Shulamith Schlick\*

Department of Chemistry, University of Detroit, Detroit, Michigan 48221.

Received October 28, 1986

**ABSTRACT:** Two types of peroxy radicals have been obtained in polypropylene by  $\gamma$  irradiation and exposure to oxygen. The radicals differ in their dynamics and stability. The stable and rigid peroxy radical can be studied separately after the decay of the mobile radical. Reversible changes in the ESR spectra from the peroxy radicals have been studied from 77 to 303 K and assigned to  $g$ -tensor averaging due to motion. The principal values of the  $g$  tensor for both radicals at 77 K are 2.0349, 2.0069, and 2.0032. ESR spectra from both radicals are simulated by using the modified Bloch equations. Best agreement with experimental results is obtained by assigning to the mobile radical a chain axis rotation with  $180^\circ$  jumps and to the rigid radical a C-O bond rotation with  $180^\circ$  jumps. The simulations indicate that the angles between  $g_1$ ,  $g_2$ , and  $g_3$  in the mobile radical and the chain axis are  $50^\circ$ ,  $97^\circ$ , and  $41^\circ$ , respectively.  $g_1$  is in the direction of the O-O bond, and  $g_3$  is perpendicular to the COO plane. Inspection of the spectra from polypropylene  $\gamma$  irradiated under vacuum suggests that the most likely precursors for the rigid and mobile peroxy radicals are the midchain radical  $-\text{CH}_2\dot{\text{C}}(\text{CH}_3)\text{CH}_2-$  and the end-chain or propagating radical  $-\text{CH}_2\text{CH}(\text{CH}_3)\text{CH}_2^\bullet$ , respectively. An additional end-chain radical,  $-\text{CH}_2\text{CH}(\text{CH}_3)$ , is also formed on  $\gamma$  irradiation. No significant effect of the degree of crystallinity on the ESR spectra or intensity ratio of the two radicals has been detected.

## Introduction

The radiation chemistry of polypropylene (PP) has been extensively investigated in recent years.<sup>1-9</sup> Samples irradiated under vacuum have indicated the presence of several alkyl radicals which have been studied by ESR spectroscopy in polypropylenes with different degrees of crystallinity. It has been suggested that most of these alkyl radicals are located in the crystalline portions of the samples, thus explaining the considerable stability of the radicals in the absence of oxygen.<sup>5,7</sup>

High-energy irradiation of PP in air, or exposure of the alkyl radicals formed under vacuum to oxygen, results in formation of peroxy radicals. These radicals were also studied by ESR and identified by their typical  $g$  anisotropy and lack of hyperfine interaction. In contrast to alkyl

radicals, however, the peroxy radicals in PP decay at room temperature within several days and even faster when the temperature is increased to 310 K. It has been suggested that peroxy radicals are localized in the amorphous regions of the polymer.<sup>5,10</sup> The kinetics of the peroxy radical decay in PP has been widely studied, because polymer oxidation results in degradation and in change in the mechanical properties on which the use of PP is based.<sup>2</sup>

ESR studies have also indicated that two types of peroxy radicals are formed in PP, with different mobilities and stabilities. The "rigid" peroxy radicals have been studied by Suryanarayana and Kevan<sup>8</sup> in terms of a specific motional mechanism. Both types of radicals have been studied by Kashiwabara and co-workers.<sup>9</sup> The main conclusions from these studies were that the mobile peroxy

radicals are localized in regions of low crystallinity and the rigid radicals are trapped in highly ordered regions of the polymer; in addition it was suggested that the intensity ratio of the two radicals and the principal values of the  $g$  tensor from the mobile radical are temperature dependent.<sup>9</sup>

We became interested in the radiation chemistry of PP because the radical species obtained in bulk PP present a clear case of reactivity being a function of mobility. We have found that ESR spectra of peroxy radicals often reflect the symmetry and microscopic structure of the medium and that comparison of calculated with experimental spectra enables determination of the specific motional mechanism.<sup>11</sup> For this reason the peroxy radicals have been utilized as spin probes in a variety of polymeric systems.<sup>11-15</sup> The use of peroxy radicals involves the averaging of the  $g$  anisotropy, which extends over a range of about 200 MHz for measurements at X-band (9 GHz), making the peroxy probe especially sensitive to fast motions. The measured ESR spectra as a function of temperature are compared with calculated spectra based on the modified Bloch equations for different values of the lifetime of the radical between the jumps.

The peroxy probe method has been applied also to the study of peroxy radicals in polyethylene.<sup>11b</sup> In this system extra lines appear in the ESR spectra of the radicals as the sample is warmed above 77 K. We have demonstrated that these lines are due to molecules for which the motional process does not much change their resonance frequency, so that exchange narrowed lines result even at low rates of motion. In our interpretation there is no need to assume drastic variations in the  $g$  values, which are very hard to justify, in order to understand the motional process. These assumptions have been made in the interpretation of the dynamics of peroxy radicals in polypropylene. As will become evident below, we propose a different approach, based on plausible assumptions.

This study was undertaken with two main objectives. First, our goal was to analyze the detailed motional mechanism in both types of peroxy radicals formed in PP. In addition, we wanted to study the effect of sample crystallinity on the ESR spectra and on the relative intensity of the two types of radicals. In order to fully analyze the results, we had to go one step back and reanalyze and simulate the spectra of the alkyl radicals obtained in PP, as possible precursors of the peroxy radicals. As a result of this study a detailed picture is obtained on the dynamics of peroxy radicals and the identity of the corresponding alkyl radicals in polypropylene.

## Experimental Section

Two polypropylene samples containing different, small, amounts of antioxidants were obtained from Hercules Inc. The samples were used as sent or purified as follows. The polymer was dissolved in boiling toluene, precipitated by and washed in acetone, and vacuum dried. This procedure was repeated 3 times. The degree of crystallinity in these polymer samples was determined by pycnometry measurements of the density in 2-propanol using established procedures.<sup>16</sup> The values of 0.935 and 0.854 g cm<sup>-3</sup> for the densities of crystalline and amorphous polypropylene, respectively, were used.<sup>17</sup> The crystallinity fractions  $X_c$  in the untreated polymer were 0.430 and 0.675. After purification the values of  $X_c$  increased to 0.651 and 0.817, respectively. This increase in crystallinity has been observed before for PP purified by solution in *n*-heptane and other hydrocarbons.<sup>18</sup> In this way four batches of polypropylene with crystallinity fractions of 0.817, 0.675, 0.651, and 0.430 were prepared. The polymer samples were transferred to 3-mm-o.d. quartz tubes, evacuated to 10<sup>-5</sup> Torr at ambient temperature, annealed at 370 K under vacuum for 36 h, and sealed under vacuum.  $\gamma$  Irradiation was carried out in a Gammacell 200 <sup>60</sup>Co source (Atomic Energy of Canada, Ltd) at

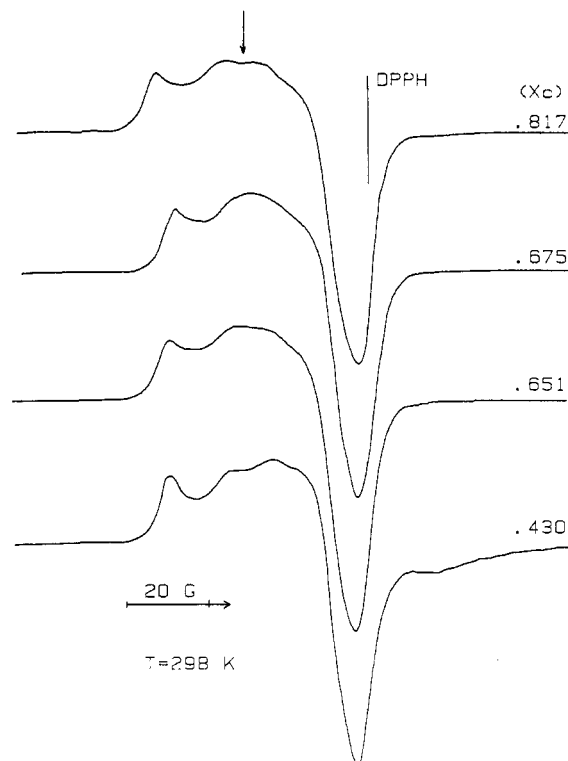


**Figure 1.** X-band ESR spectra of peroxy radicals in polypropylene at 298 K for the indicated crystallinity fractions  $X_c$ . Total dose: 30 Mrad. The arrow indicates extra signals, due to motional averaging of the  $g$  anisotropy.

a dose rate of 1.25 Mrad h<sup>-1</sup> at the University of Houston to a total dose of ~30 Mrad or at a dose rate of 0.05 Mrad h<sup>-1</sup> to a total dose of 1–6 Mrad at Oakland University, at ambient temperature. The corresponding peroxy radicals were obtained by exposing the samples to air.

ESR spectra were measured at X-band with a Varian E-9 spectrometer operating at 9.3 GHz and with a Bruker 200D SRC spectrometer operating at 9.7 GHz, using 100-kHz modulation. Spectra at 77 K were taken in a liquid nitrogen Dewar inserted in the ESR cavity. In the range 96–300 K ESR spectra were measured with the Bruker ER 4111 variable temperature unit with liquid nitrogen as coolant in a flow system. The temperature of the sample was measured by a digital chromel-constantan thermocouple with an accuracy better than  $\pm 2$  K. The absolute value of the magnetic field was measured with the Bruker ER 035 M NMR gaussmeter. Calibration of  $g$  values was based on DPPH ( $g = 2.0036$ ) and <sup>53</sup>Cr<sup>3+</sup>-doped MgO single crystals ( $g = 1.9800$ ). The scan of the Varian spectrometer was calibrated with <sup>55</sup>Mn<sup>2+</sup>-doped MgO single crystals. The value of 86.7 G for the separation of the two center lines of the hyperfine sextet was used. When using the Bruker spectrometer, direct field readings were used for scan measurement.

Computer simulations of ESR spectra were performed on a Burroughs 6800 mainframe computer and were plotted by using an IBM PC and a Hewlett-Packard 7470A digital plotter. ESR spectra of peroxy radicals were calculated with the codes we developed, based on the modified Bloch equations.<sup>11</sup> ESR spectra of alkyl radicals were calculated with the code written by Paul Kasai of IBM Instruments.<sup>19</sup>

## Results

**ESR Spectra.** Peroxy radicals in polypropylene were obtained by  $\gamma$  irradiation under vacuum followed by exposure to air and were studied in the temperature range 77–313 K. Typical ESR spectra are shown in Figures 1–4. Figure 1 gives ESR spectra of the peroxy radicals as a function of the degree of crystallinity of the polymer, at 298 K. No significant variations in the lineshapes are detected in these spectra. ESR spectra of peroxy radicals obtained in PP with  $X_c = 0.675$  are shown in Figure 2 in

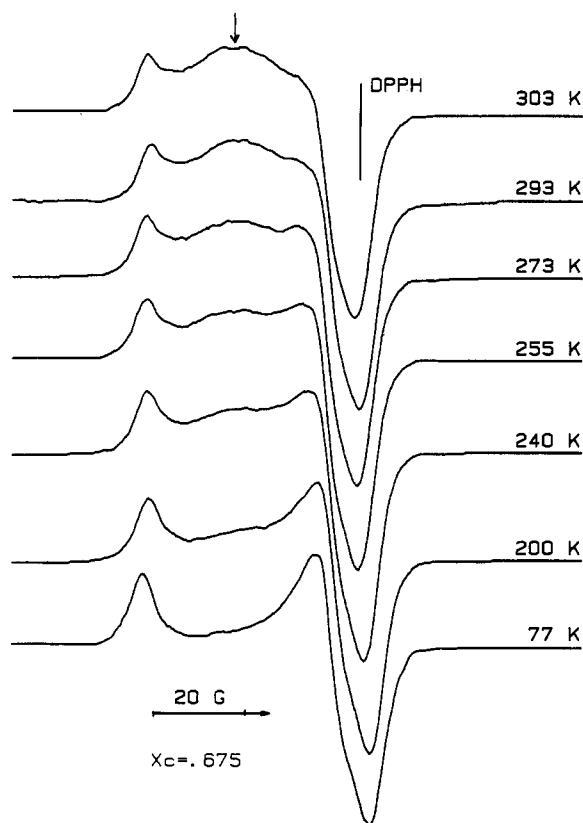


**Figure 2.** X-band ESR spectra of peroxy radicals in polypropylene with  $X_c = 0.675$  at the indicated temperatures. Total dose: 28 Mrad. Spectra were taken immediately after exposure to air and disappearance of alkyl radicals. The arrow indicates extra signals, due to motional averaging of the  $g$  anisotropy.

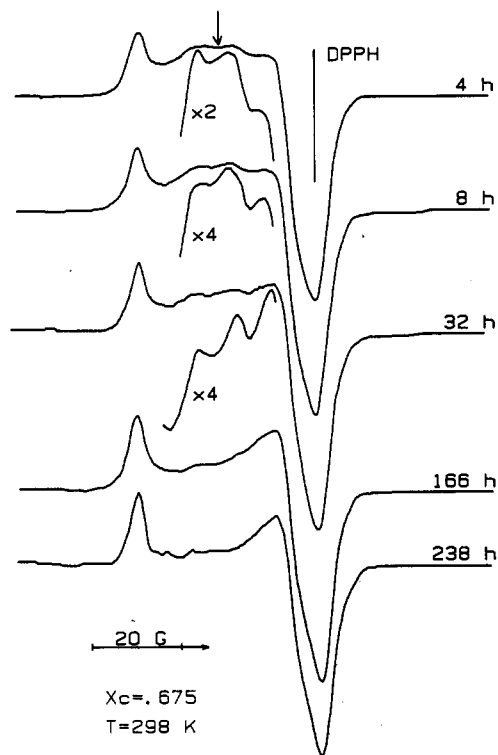


**Figure 3.** X-band ESR spectra at 298 K of peroxy radicals in polypropylene with  $X_c = 0.675$  after the indicated times of exposure to air. Total dose: 28 Mrad. The arrow indicates extra signals, due to motional averaging of the  $g$  anisotropy.

the temperature range 77–303 K. Figure 3 indicates the disappearance of one type of peroxy radicals as a function of time, at 298 K. This less stable peroxy radical represents

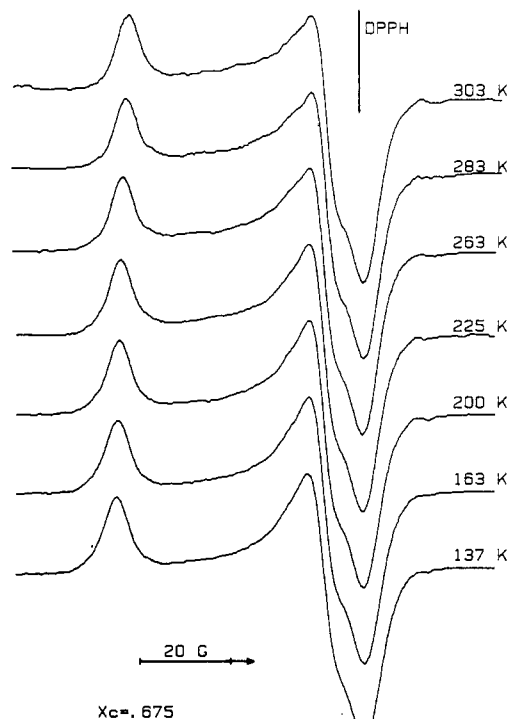


**Figure 4.** X-band ESR spectra of peroxy radicals in polypropylene irradiated to a total dose of 3.7 Mrad, at the indicated temperatures. The spectra were taken after complete decay of the mobile radicals by heating at 313 K for 2 h.

the mobile radical; the remaining signal belongs to the rigid radical. Figure 4 shows the lineshape as a function of temperature for the rigid radical, after complete decay of the mobile component.

The results presented in Figures 2–4 very clearly indicate the presence of the two types of peroxy radicals in PP. The rigid radical can be studied separately, as shown in Figure 4, after the decay of the mobile radical. The extra transitions, indicated by arrows in these figures, clearly are due to the mobile radicals because they are absent in Figure 4.

In all the measured spectra we have not detected any significant effect of the irradiation dose or of the small amount of antioxidant in the samples on the ESR lineshapes or on the relative intensity of the two peroxy radicals.

**Simulations.** To interpret the temperature variation of the ESR spectra, we compare the experimental results with spectra calculated by using the modified Bloch equations, as a function of jump rate  $\tau^{-1}$  of the radical between the possible sites.<sup>11</sup> The calculation of the spectra involves the evaluation of the transformation matrix of the  $g$  tensor for the particular model chosen and depends upon the geometrical relationship between the sites in each case.

On the basis of the appearance of the spectra and previous studies,<sup>14</sup> we have used two models of rotation for the two types of radicals present in the spectra. The C–O bond rotation model with the O–O group undergoing 180° jumps has been successfully used before to simulate the ESR spectra of the rigid peroxy radical.<sup>8</sup> Good agreement has been obtained with a COO angle of 104°.

A different model must be used to simulate the spectra of the less stable and more mobile peroxy radical. We have extensively studied various models of chain axis rotation in order to simulate exactly the experimental position and intensity of the “extra” lines that appear at intermediate temperatures in Figures 1–3. The model that best reproduces the experimental results is shown in Figure 5a. The

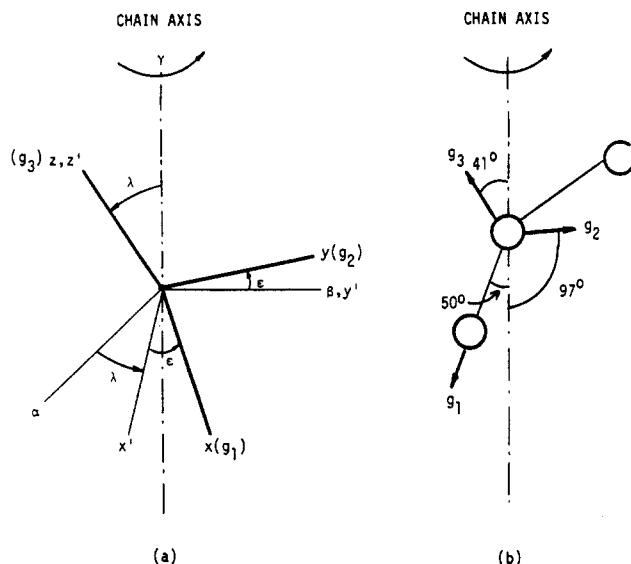


**Figure 5.** (a) Model of the chain axis rotation used for simulation of ESR spectra from the mobile peroxy radicals in polypropylene. (b) Orientation of  $g_1$ ,  $g_2$ , and  $g_3$  with respect to the polymer chain axis, deduced from the values of  $\lambda$  and  $\epsilon$  used for the simulation that best reproduces the experimental results.

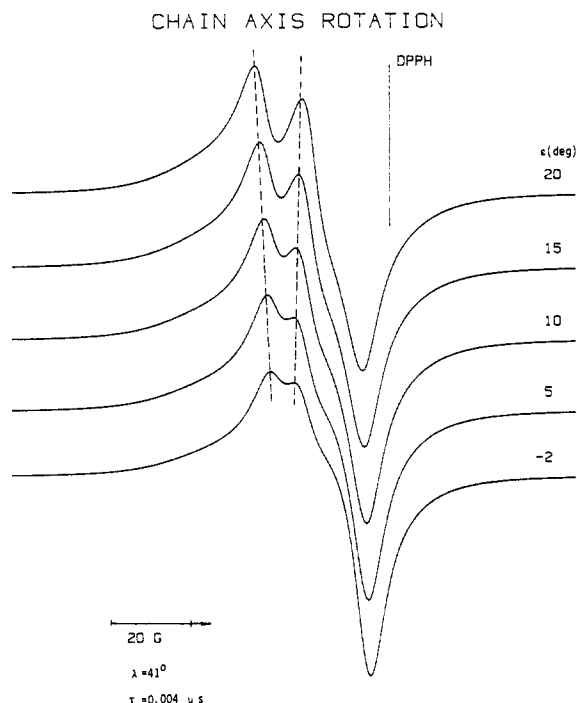


**Figure 6.** Effect of the value of  $\epsilon$  on the ESR lineshapes calculated with the model shown in Figure 5a with a constant  $\lambda$  value of  $41^\circ$ , for  $\tau = 0.004 \mu s$ . A constant intrinsic line width of 13 MHz, independent of orientation, was maintained in all simulations.

motional model is a chain axis rotation; the orientation of the principal values of the  $g$  tensor from the peroxy radicals with respect to the direction of the chain axis is specified by the angles  $\lambda$  and  $\epsilon$ . In Figure 5a  $g_1$  is the direction of the O-O bond and  $g_3$  is perpendicular to the COO plane. All spectra were calculated with the  $g$  values deduced from ESR spectra at 77 K:  $g_1 = 2.0349$ ,  $g_2 = 2.0069$ , and  $g_3 = 2.0032$ .

The values of  $\lambda$  and  $\epsilon$  control the position and intensities of the extra lines which are observed experimentally. The sensitivity of the calculated spectra to the values of these angles is clearly indicated in Figures 6 and 7, which represent simulated spectra for the mobile peroxy radical. Pairs of values of  $\lambda$  and  $\epsilon$  determine the final geometry of

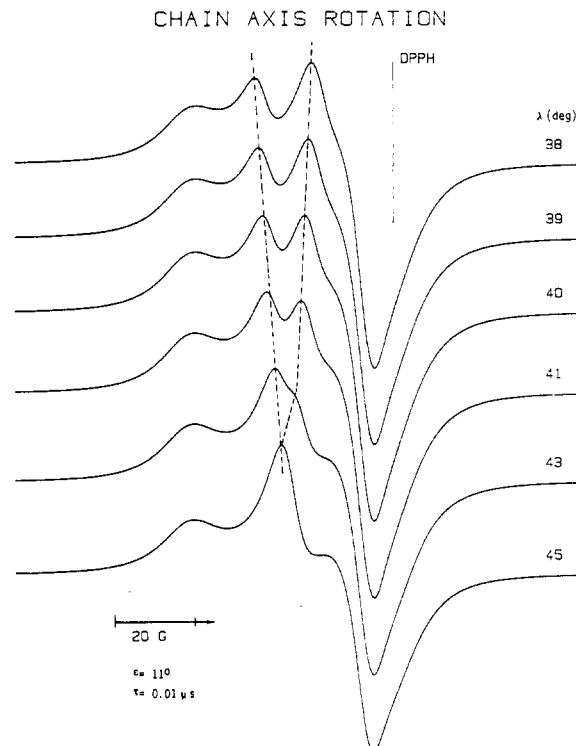


**Figure 7.** Effect of the value of  $\lambda$  on the ESR lineshapes calculated with the model shown in Figure 5a with a constant  $\epsilon$  value of  $11^\circ$ , for  $\tau = 0.01 \mu s$ . A constant intrinsic line width of 13 MHz, independent of orientation, was maintained in all simulations.

the peroxy fragment COO and the angles of the three components of the  $g$  tensor with respect to the chain axis.

In calculating all spectra we have also introduced for both models a variation of the intrinsic line width with orientation

$$(\Delta H)^2 = (\Delta H_1)^2 \sin^2 \theta \cos^2 \phi + (\Delta H_2)^2 (\sin^2 \theta \sin^2 \phi + \cos^2 \theta)$$

$\Delta H$  is the orientation-dependent line width,  $\Delta H_1$  is the line width along the direction of  $g_1$  and  $\Delta H_2$  is the line width along  $g_2$  and  $g_3$ ;  $\theta$  and  $\phi$  specify the orientation of the external magnetic field relative to the principal values of the  $g$  tensor.

Simulation of the experimental spectra containing contributions from both peroxy radicals was accomplished by superposition of the contribution from the rigid peroxy radical, calculated with the CO bond rotation model with  $180^\circ$  jumps, and from the mobile radical, calculated from the chain axis rotation model with  $180^\circ$  jumps, with the geometry shown in Figure 5a. In Figure 8 are separately shown the calculated spectra for the two models of rotation, before superposition. From Figure 8 we can clearly visualize the effects of the superposition on the resulting spectra, as the value of  $\tau$  decreases. The shift of  $g_3$  toward lower field and the appearance of extra transitions are due to the chain axis rotation of the mobile radical. The small upfield shift of  $g_1$  is due to the C-O bond rotation of the rigid radical. These effects duplicate the experimentally observed changes in the ESR spectra with increase in temperature, as shown in Figures 1-4.

Figure 9 is the superposition of the mobile and rigid radicals with a constant intensity ratio of 0.95:1. In this final simulation, we use  $\lambda = 41^\circ$  and  $\epsilon = 11^\circ$ . In spite of the many parameters involved in the superposition of two simulated spectra, the agreement between the calculated spectra in Figure 9 and experimental results shown in Figure 2 is very satisfactory. We used a constant intensity

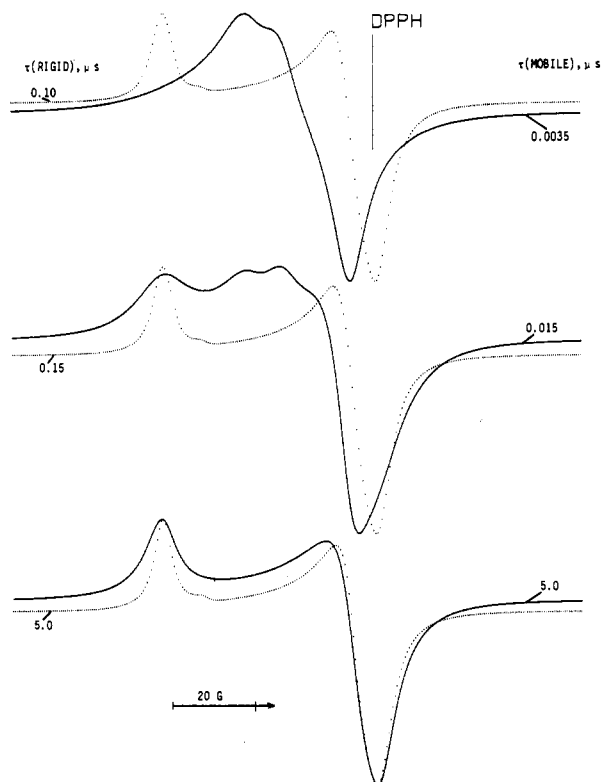


**Figure 8.** Simulated lineshapes for the mobile and rigid peroxy radicals in polypropylene. In all simulations we used  $g_1 = 2.0349$ ,  $g_2 = 2.0069$ ,  $g_3 = 2.0032$ , and an intrinsic line width variation with orientation:  $\Delta H_1 = 23$  MHz,  $\Delta H_2 = 13$  MHz for the mobile radical, and  $\Delta H_1 = 7$  MHz,  $\Delta H_2 = 12$  MHz for the rigid radical. The solid line indicates the simulation of ESR spectra from the mobile radicals, based on the chain axis rotation with  $180^\circ$  jumps as shown in Figure 5a, with  $\lambda = 41^\circ$  and  $\epsilon = 11^\circ$ . The dotted line represents the simulation of ESR spectra from the rigid peroxy radicals, using a C-O bond rotation model with  $180^\circ$  jumps, with a COO angle of  $104^\circ$ , as in ref 8.

ratio of the two radicals because during the time of the experiment there is no measurable change in the intensity ratio of the two peroxy radicals.

From the values of  $\lambda$  and  $\epsilon$  used for the simulation shown in Figure 9 we determined the orientation of the principal values of the  $g$  tensor for the mobile radical, relative to the polymer chain direction. The angles are  $50^\circ$ ,  $97^\circ$ , and  $41^\circ$  for  $g_1$ ,  $g_2$ , and  $g_3$ , respectively, and are indicated in Figure 5b.

### Discussion

As seen from Figure 1, the degree of crystallinity has no significant effect on the ESR spectra of the peroxy radicals. The slight variation in lineshape detected and shown in Figure 1 is most likely due to the different stage of decay of the mobile radical in each of the spectra shown. The simulation of the mobile radical shown in Figures 6–8 indicates that two extra lines appear as a result of motion. The line widths detected in ESR spectra are, in general, a function of the radical concentration, and all lines are expected to be narrower when some of the radicals have decayed, including the extra lines.

In addition, a certain degree of heterogeneity in the trapping sites for the peroxy radicals is also expected, due to the complex morphology of polymeric systems. This heterogeneity is expected to decrease if some radicals decay, also leading to narrower lines. The slight lineshape variations shown in Figure 1 and also detected in a previous study<sup>9</sup> are most likely due to these two effects.

The observation of two peroxy radicals with different motional mechanisms has been observed before in Teflon<sup>12</sup>

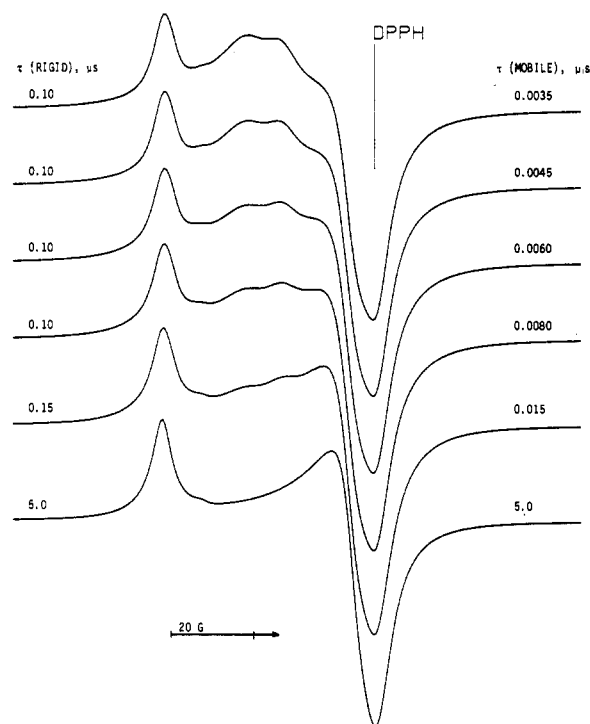


**Figure 9.** Superposition of spectra shown in Figure 8, with an intensity ratio of 0.95 between the mobile and the rigid radicals.

and assigned to different radical structures. PP is unique because the radicals have different dynamics and chemical stability. The stability must be related not only to the polymer morphology but also to the location of the peroxy group in the chain. The fact that the degree of crystallinity does not seem to affect greatly the lineshapes and the intensity ratio of the two radicals indicates that the structure of the radical is the dominant factor in the radical stability. Therefore it is important to study the alkyl radicals produced in PP as precursors of the peroxy radicals.

The radical that is believed to dominate the ESR spectrum of  $\gamma$ -irradiated PP at ambient temperature is the midchain radical  $-\text{CH}_2\dot{\text{C}}(\text{CH}_3)\text{CH}_2-$ . The ESR spectrum of this radical has been described in terms of the "8 line spectrum" or the "15 line spectrum" by various authors.<sup>1,2,20,21</sup> The simulation of the spectrum has been attempted by assuming seven identical protons with an isotropic hyperfine splitting of 23 G and line width of 20 G.<sup>20</sup> It is important to note that in this interpretation strong lines are not expected in the center of the spectra.

The ESR spectrum of the  $\gamma$ -irradiated PP under vacuum to a total dose of 2 Mrad obtained in this study is shown in Figure 10a. The resolution we obtained at low irradiation doses is very good and the line width is 6 G peak to peak. A strong line, whose intensity is a function of the time elapsed after the irradiation, is observed in the center of the symmetrical spectrum. This variation is presented in Figure 10b. Figure 10c shows the ESR spectrum measured 20 days after the irradiation; it is clear that most of the intensity in the wings is lost. In Figure 10d we present the result of the subtraction of spectra 10a and 10b; the result very closely duplicates the experimental spectrum shown in Figure 10c, indicating the presence of at least two radicals in the irradiated polymer.

The lines in the wings of the experimental spectra, Figure 10, parts a and b, are well simulated by assuming the presence of the midchain radical  $-\text{CH}_2\dot{\text{C}}(\text{CH}_3)\text{CH}_2-$  with proton hyperfine splittings of 21.8 (5 protons) and 30.0 G (2 protons), as shown in Figure 11a. The peroxy

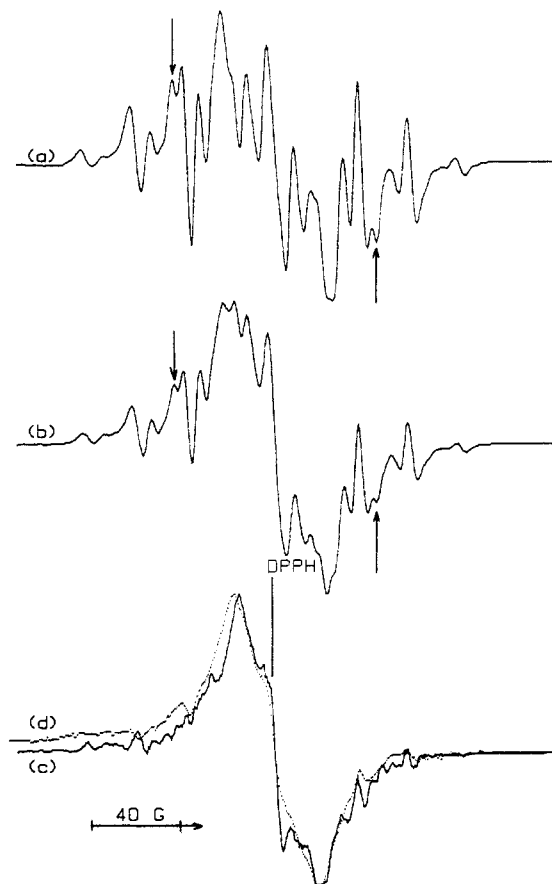
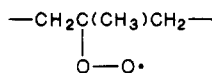


**Figure 10.** ESR spectra of radicals obtained by  $\gamma$  irradiation of polypropylene in the absence of air, at 298 K. Total dose is 2 Mrad in (a) and 3 Mrad in (b). In (c) we present ESR spectrum observed 20 days after  $\gamma$  irradiation. (d) Subtraction of ESR spectra from (a) and (b).

radical corresponding to this alkyl radical has been prepared by Faucitano et al.<sup>20</sup> and was shown to have great stability. We therefore suggest that the stable and rigid peroxy radical measured in this study is obtained from the alkyl midchain radical and has the structure



This assignment is in good agreement with the reduced mobility observed before for chain peroxy radicals in a series of polymers with substituted chains, such as methacrylates.<sup>8</sup> In these radicals, as in the rigid PP peroxy radical in this study, the only motion that simulates well the experimental results is a C-O bond rotation.

The line observed in the center of the spectrum in Figure 10 parts a and b, must belong to an additional alkyl radical. The presence of allyl or polyenyl peroxy radicals has been suggested<sup>22</sup> and these radicals contribute a broad line in the spectrum center, in agreement with Figure 10. Another possibility is suggested by the ESR spectra shown in Figure 10, parts c and d, which have a total width of  $\sim 70$  G. This splitting might be due to the end-chain radical  $\text{---CH}_2\text{CH}(\text{CH}_3)\text{CH}_2\cdot$ , with hyperfine splittings of 20 G for the two  $\alpha$ -protons and 30 G for the  $\beta$ -proton. The superposition of this propagating radical, Figure 10d, and the midchain radical  $\text{---CH}_2\text{C}(\text{CH}_3)\text{CH}_2\cdot$  is shown in Figure 11b; the important features in the experimental spectra are well reproduced in this spectrum, except the lines marked by arrows in Figure 10a. These lines might be due to an additional alkyl radical. We suggest the radical  $\text{---CH}_2\dot{\text{C}}\text{HCH}_3$ , which is an *end-chain* radical. The simu-

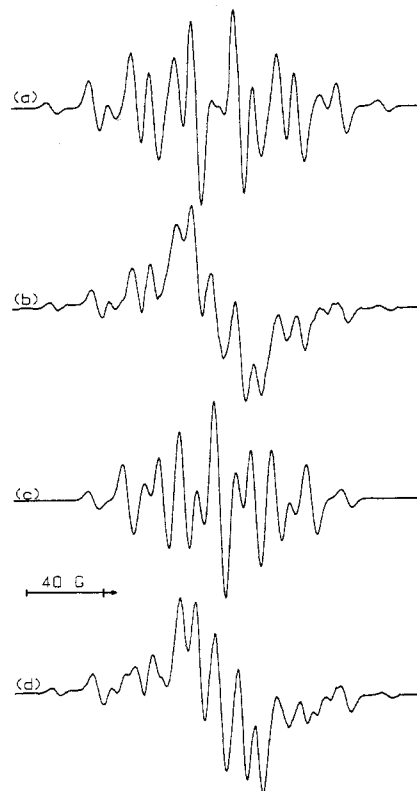


**Figure 11.** (a) Computer simulation of the ESR spectrum from the midchain alkyl radical  $\text{---CH}_2\dot{\text{C}}(\text{CH}_3)\text{CH}_2\text{---}$ , with hyperfine splittings of 21.8 (5 protons) and 30.0 G (2 protons), Gaussian lineshapes, and a peak-to-peak derivative line width of 6.4 G. (b) Superposition of the midchain alkyl radical in part a with the end-chain radical in Figure 10d, in a ratio of 0.48:1. (c) Computer simulation of the ESR spectrum from the end-chain radical  $\text{---CH}_2\dot{\text{C}}\text{H}(\text{CH}_3)$ , with hyperfine splittings of 28.5 G from two  $\beta$ -protons and 18 G from the  $\alpha$ -proton and the methyl protons, Gaussian lineshapes, and a peak-to-peak derivative line width of 5.8 G. (d) Superposition of ESR spectra shown in Figures 11a,c and 10d in a ratio of 0.35:1:0.37.

lated ESR spectrum of this radical is shown in Figure 11c, based on hyperfine splittings of 28.5 G from two  $\beta$ -protons and 18 G from the  $\alpha$ -proton and the three protons of the methyl group. The superposition of the chain radical (Figure 11a), the propagating radical (figure 10d), and the propagating radical (Figure 11c) is shown in Figure 11d. In this spectrum all lines experimentally observed are reproduced. Exact simulation of the spectra shown in Figure 10, parts a and b, is very difficult, because the overall lineshape is very sensitive to small differences in the hyperfine splittings. Small differences in the  $g$  values of the radicals considered are also possible and are probably responsible for the slight asymmetry in the experimental spectra. We detected variations in the lineshape as a function of the irradiation dose, and this confirms our suggestion that several alkyl radicals are obtained in PP, with very similar stabilities, making the separation process impossible.

The two propagating radicals considered in the final simulated spectra, Figure 11d, are very likely precursors of the mobile peroxy radical detected in this study, to which a chain axis rotation has been assigned. We have observed this type of motion in a variety of end-chain peroxy radicals, in contrast to the more limited mobility of chain peroxy radicals.<sup>11</sup>

## Conclusions

1. Two peroxy radicals, with different stabilities and motional processes, are formed when  $\gamma$ -irradiated PP is

exposed to air. The principal values of the  $g$  tensor for both radicals are 2.0349, 2.0069, and 2.0032 at 77 K. Extra transitions are observed due to motional averaging.

2. The relative intensity of and the lineshapes from these radicals are not sensitive to the degrees of crystallinity of the polymer in the range 0.430–0.817.

3. The more stable peroxy radical is a chain radical whose precursor is the midchain alkyl radical  $-\text{CH}_2\dot{\text{C}}(\text{CH}_3)\text{CH}_2-$ .

4. The temperature dependence of the ESR spectra from the mobile peroxy radical is simulated well by assuming a chain axis rotation with  $180^\circ$  jumps. The angles between the principal values of the  $g$  tensor and the chain axis are  $50^\circ$ ,  $97^\circ$ , and  $41^\circ$  for  $g_1$ ,  $g_2$ , and  $g_3$ , respectively. Likely precursors for this peroxy radical are the propagating radicals  $-\text{CH}_2\dot{\text{C}}\text{H}(\text{CH}_3)$  and  $-\text{CH}_2\dot{\text{C}}\text{H}(\text{CH}_3)\text{CH}_2\cdot$ .

**Acknowledgment.** We thank Dr. E. J. Vandenberg of Hercules for the sample of polypropylene. This research was supported by a grant from the Research Corp., by the University of Detroit, and by an NSF Instrumentation Grant DMR-8501362 for the purchase of the ESR spectrometer.

**Registry No.** PP, 9003-07-0.

## References and Notes

- (1) Geimer, D. O. In *The Radiation Chemistry of Macromolecules*; Dole, M. Ed.; Academic: New York, 1973; Chapter 1.
- (2) Gvozdk, N.; Basheer, R.; Mehta, M.; Dole, M. *J. Phys. Chem.* 1981, 85, 1563.
- (3) (a) Garton, A.; Carlsson, D. J.; Wiles, D. M. *Macromolecules* 1979, 12, 1071. (b) Carlsson, D. J.; Dobbin, C. J. B.; Wiles, D. M. *Macromolecules* 1985, 18, 1791.
- (4) Chien, J. C. W.; Boss, C. R. *J. Polym. Sci., Part A-1* 1967, 5, 1683, 3091.
- (5) Nunome, K.; Eda, B.; Iwasaki, M. *J. Appl. Polym. Sci.* 1974, 18, 2719.
- (6) Reuben, J.; Mahlman, B. H. *J. Phys. Chem.* 1984, 88, 4904.
- (7) Bartos, J.; Tino, J. *Collect. Czech. Chem. Commun.* 1985, 50, 1391.
- (8) Suryanarayana, D.; Kevan, L. *J. Phys. Chem.* 1982, 86, 2042.
- (9) (a) Hori, Y.; Makino, Y.; Kashiwabara, H. *Polymer* 1984, 25, 1436. (b) Shimada, S.; Kotake, A.; Hori, Y.; Kashiwabara, H. *Macromolecules* 1984, 17, 1104. (c) Hori, Y.; Shimada, S.; Kashiwabara, H. *J. Polym. Sci., Polym. Phys. Ed.* 1984, 22, 1407. (d) Shimada, S.; Hori, Y.; Kashiwabara, H. *Macromolecules* 1985, 18, 170.
- (10) Szocz, F. *J. Appl. Polym. Sci.* 1982, 27, 1865.
- (11) Schlick, S.; Kevan, L. *J. Phys. Chem.* 1979, 83, 3424; *J. Am. Chem. Soc.* 1980, 102, 4622; *J. Phys. Chem.* 1986, 90, 1998.
- (12) Suryanarayana, D.; Kevan, L.; Schlick, S. *J. Am. Chem. Soc.* 1982, 104, 668.
- (13) Schlick, S.; McGarvey, B. R. *J. Phys. Chem.* 1983, 87, 352.
- (14) Schlick, S.; Chamulitrat, W.; Kevan, L. *J. Phys. Chem.* 1985, 89, 4278.
- (15) Suryanarayana, D.; Chamulitrat, W.; Kevan, L. *J. Phys. Chem.* 1982, 86, 4822.
- (16) ASTM D-792-66 (75).
- (17) Choy, C. L.; Leung, W. P.; Ma, T. L. *J. Polym. Sci., Polym. Phys. Ed.* 1985, 23, 557.
- (18) Knight, J. B.; Calvert, P. D.; Billingham, N. C. *Polymer* 1985, 26, 1713.
- (19) (a) Kasai, P. H. *J. Am. Chem. Soc.* 1972, 94, 5950. (b) Kasai, P. H.; McLeod, D., Jr.; McBay, H. C. *J. Am. Chem. Soc.* 1974, 96, 6864. (c) Kasai, P. H. *J. Phys. Chem.* 1986, 90, 5034.
- (20) Fautitano, A.; Buttafava, A.; Martinotti, F.; Gratani, F.; Bortolus, P. *J. Polym. Sci., Polym. Chem. Ed.* 1985, 23, 635.
- (21) Fischer, H.; Hellwege, K. H. *Polym. Lett.* 1966, 4, 503.
- (22) Dunn, T. S.; Epperson, H. W.; Stannett, V. T.; Williams, J. L. *Radiat. Phys. Chem.* 1979, 14, 625.

## <sup>13</sup>C NMR Study of the Selectivity in the Modification of Dextran with Ethyl Chloroformate

Félix Arranz,\* Julio San Román, and Manuel Sánchez-Chaves

Instituto de Plásticos y Caucho, 28006 Madrid, Spain. Received July 24, 1986

**ABSTRACT:** The selectivity of the reaction of dextran with ethyl chloroformate in the homogeneous phase has been studied by <sup>13</sup>C NMR. The analysis of spectra of the anhydroglucose, oxymethylene, and carbonyl carbons shows that the hydroxyl group at position C-2 is selectively substituted and that the reactivity of individual secondary hydroxyls decreases in the order C-2 > C-4 > C-3. The results obtained are explained by considering the formation of intramolecular hydrogen bonding between the hydroxyl at C-2 and the axial anomeric oxygen as well as between the hydroxyl at C-4 and the carbonyl group of the ethyl carbonate at the C-2 position on the adjacent anhydroglucose unit.

## Introduction

It is well-known that the degree of substitution (DS) of polysaccharides may have important effects on their behavior and properties. However, derivatives with similar DS values may have different substituent distributions. The difference in the relative DS at individual hydroxyl groups arises from the fact that three hydroxyl groups at the anhydroglucose residue may differ in reactivity.<sup>1-3</sup> The physical, chemical, and biochemical properties are considered to depend markedly on the distribution of substituents in the anhydroglucose units.<sup>4-7</sup>

The relative reactivities of these groups have been investigated mainly by chemical methods.<sup>8-10</sup> However, at present <sup>1</sup>H and <sup>13</sup>C NMR spectroscopy have afforded more accurate knowledge of structures, with a consequent increase in the reliability of deductions based on them. Recently, the study of the microstructural characterization

of cellulose acetates by <sup>13</sup>C NMR<sup>7,11,12</sup> has been suggested. The distribution of *O*-acetyl groups can be estimated not only from the *O*-acetyl carbonyl carbon spectra but also from the ring carbon spectra.

In general, the models used to study the substitution reactions in cellulose and other polysaccharides involve the following assumptions:<sup>5,13-15</sup> (a) all the anhydroglucose units in the polysaccharide molecule are equally accessible for reaction; (b) the relative rate constants of reaction of the different hydroxyls remain unchanged throughout the process; (c) substitution within a given unit does not affect the reactivity of the remaining unreacted hydroxyls; and (d) the effects of end groups are negligible.

On the other hand, dextrans are high molecular weight polymers of D-glucopyranose synthesized from sucrose by a number of bacterial species belonging to the family Lactobacillae. Most of the glucosidic linkages are 1→6,